ISSN 0021-3640, JETP Letters, 2015, Vol. 102, No. 6, pp. 355–360. © Pleiades Publishing, Inc., 2015.
Original Russian Text © V.G. Myagkov, V.S. Zhigalov, L.E. Bykova, G.N. Bondarenko, A.N. Rybakova, A.A. Matsynin, I.A. Tambasov, M.N. Volochaev, D.A. Velikanov, 2015, published in Pis'ma v Zhurnal Eksperimental'noi i Teoreticheckoi Fiziki, 2015, Vol. 102, No. 6, pp. 393–398.

CONDENSED MATTER

High Rotatable Magnetic Anisotropy in Epitaxial $L1_0$CoPt(111) Thin Films

V. G. Myagkov[a, *], V. S. Zhigalov[a, b], L. E. Bykova[a], G. N. Bondarenko[c], A. N. Rybakova[a, b], A. A. Matsynin [a, d], I. A. Tambasov[a], M. N. Volochaev[a, b], and D. A. Velikanov[a, d]

[a] *Kirensky Institute of Physics, Siberian Branch, Russian Academy of Sciences, Krasnoyarsk, 660036 Russia*
[b] *Reshetnev Siberian State Aerospace Krasnoyarsk, Krasnoyarsk, 660014 Russia*
[c] *Institute of Chemistry and Chemical Technology, Siberian Branch, Russian Academy of Sciences, Krasnoyarsk, 660036 Russia*
[d] *Siberian Federal University, Krasnoyarsk, 660041 Russia*
** e-mail: miagkov@iph.krasn.ru*

Received June 15, 2015

The evolution of the structural and magnetic properties in epitaxial film systems Co/Pt(111) of equiatomic composition during vacuum annealing has been presented. Annealing to the temperature of 400°C does not lead to the variation of the structural and magnetic properties of the films, which indicates the absence of considerable mixing of the Co/Pt interface. With the increase in the annealing temperature from 400 to 750°C, nanoclusters containing the main magnetically hard $L1_0$CoPt(111) phase epitaxially intergrown with the $CoPt_3$ phase are formed. High rotatable magnetic anisotropy has been found in the prepared films. In magnetic fields above the coercive force ($H > H_C = 8$ kOe), the easy anisotropy axis with the angle of lag taken into account can be oriented in any spatial direction. Possible mechanisms of the formation of the rotatable magnetic anisotropy have been discussed. It has been assumed that the high rotatable magnetic anisotropy makes the main contribution to the magnetic perpendicular anisotropy in Co_xPt_{1-x} films.

DOI: 10.1134/S0021364015180101

INTRODUCTION

The structural and magnetic properties of thin films ordered according to the $L1_0$ type (FePd, FePt, CoPt) and having a large magnetocrystalline anisotropy constant ($K_1 > 10^7$ erg/cm^3) with the easy anisotropy axis coinciding with the *c* axis are widely studied in view of the potential possibility of their usage for high-density magnetic recording of information and creating special magnetic media [1, 2]. The necessary condition for the formation of thin-film media with perpendicular magnetic anisotropy is the oriented growth of $L1_0$(001) crystallites with the *c* axis coinciding with the normal to the substrate and the constant $K_U = K_1 - 2\pi M_S^2 > 0$ ($2\pi M_S^2$ is the anisotropy of the sample shape). Many studies are directed to the preparation of $L1_0$(001) thin films near the equiatomic composition by the epitaxial growth on MgO(001) substrates. Epitaxial $L1_0$CoPt(001) samples demonstrate a quite high perpendicular magnetic anisotropy constant ($K_U \sim (1–4) \times 10^7$ erg/cm^3) [3]. The epitaxial hexagonal close-packed Co_3Pt(002) [4] and $L1_1$-CoPt(111) films deposited on the (111) Pt surface have almost the same perpendicular magnetic anisotropy constant [5]. In addition to the equiatomic composition, the perpendicular magnetic anisotropy is observed in Co_xPt_{1-x} in a wide concentration range, in which the disordered fcc [6] and ordered $L1_2$-Co_3Pt [7] and $L1_2$-$CoPt_3$ [8] phases are formed. However, owing to the cubic symmetry of phases, the existence of perpendicular anisotropy in these films is not expected. The mechanisms of the appearance of perpendicular magnetic anisotropy in Co_xPt_{1-x} films deposited on amorphous substrates are also unclear [9]. In addition to the magnetocrystalline nature, different models explaining the origin of giant perpendicular magnetic anisotropy are proposed, e.g., the formation of the column structure, the preferable location of the Co–Pt bonds perpendicular to the substrate, the existence of the planar stresses, etc. However, the real nature of the perpendicular magnetic anisotropy observed in Co_xPt_{1-x} films remains unclear.

In this work, we present the first observations of the high rotatable magnetic anisotropy in Co_xPt_{1-x} films obtained by the solid-state reaction of elemental Co and Pt layers. The rotatable magnetic anisotropy was discovered in the studies of magnetism in thin films. This anisotropy means that the easy axis follows the direction of the magnetic field (see, e.g., [10]). Unlike

other kinds of anisotropies, the rotatable magnetic anisotropy is not described by a sinusoidal law and, therefore, has no unambiguous characteristic. The difference $H^{rot} = H_k^{dyn} - H_k^{stat}$ between the dynamic field of the magnetic anisotropy H_k^{dyn} measured by ferromagnetic resonance and the static field of the magnetic anisotropy H_k^{stat} is used to characterize the rotatable magnetic anisotropy [11]. In torque measurements, the rotatable magnetic anisotropy can be characterized by the average torque value L^{rot} at large rotational angles of the magnetic field (see Fig. 3). The rotatable magnetic anisotropy is observed both in magnetically soft films ($H_C < 500$ Oe) having $L^{rot} \sim (10^3–10^4)$ erg/cm^3 and $H^{rot} < 500$ Oe [12–14] and in magnetically hard materials ($H_C > 5$ kOe) with $L^{rot} \sim (10^5–10^6)$ erg/cm^3 [15, 16]. The literature review shows that the source of the rotatable magnetic anisotropy can be associated with the existence of the stripe domain structure [12], exchange interaction between the antiferromagnetic and ferromagnetic grains [13], magnetostriction [14], and freezing of correlations between spins [15]. However, there is no conventional interpretation of the rotatable magnetic anisotropy mechanisms. Our studies demonstrate that rotatable magnetic anisotropy is formed in all Co_xPt_{1-x} films with $x = 0.2–0.6$ prepared by solid-state synthesis. In this work, we present only data for epitaxial CoPt(111)/MgO(001) films of the equiatomic composition.

SAMPLES AND EXPERIMENTAL TECHNIQUE

The epitaxial Co/Pt(111) films prepared by the subsequent deposition of Pt and Co on the (001) surface of the MgO substrate were used in experiments. The deposition of the Pt layer was performed at a pressure of 10^{-6} Torr and a temperature of 250°C and led to the oriented growth of Pt(111)/MgO(001). The epitaxial growth of Pt(111) films prepared by magnetron sputtering was observed at temperatures on the Mg(001) surface up to 300°C [17]. The upper Co layer was deposited at room temperature in order to avoid the reaction of Pt with Co. The thicknesses of the reacting Co and Pt layers, which were determined by the X-ray spectral fluorescent method, were 100 and 140 nm, respectively, ensuring the equiatomic composition. The initial Co/Pt(111)/MgO(001) samples were annealed for 30 min from 300 to 750°C with a step of 50°C. The formed phases were identified on a DRON-4-07 diffractometer (CuK_α radiation). The X-ray studies of epitaxial ratios between MgO(001), reacting Pt, Co films, and the CoPt layer formed in the reaction products were performed on a PANalytikal X'Pert PRO diffractometer with a PIXctl detector. The CuK_α radiation monochromatized by a secondary graphite monochromator was used in the instrument. The saturation magnetization M_S and the coercivity H_C were measured on a vibrational magnetometer in magnetic fields up to 30 kOe. Torque curves were measured on a torque magnetometer with the maximum magnetic field of 10 kOe. All measurements were performed at room temperature.

EXPERIMENTAL RESULTS

Figure 1 shows the dependence $H_C(T)$ of the coercivity H_C in the Co/Pt(111) sample plane on the annealing temperature T. With the increase in the temperature, the initial value $H_C \sim 50$ Oe first did not change and then increased sharply after 400°C. This indicates the beginning of the strong mixing of the Co and Pt layers and the formation of magnetically hard compounds. Above 600°C, the coercivity reached $H_C \sim 8$ kOe and further only slightly increased, which indicates the complete mixing of layers and the termination of the solid-state reaction between Co and Pt.

The diffraction patterns of the initial two-layer Co/Pt(111) films contain the strong reflection from Pt(111), Pt(222) and weak peaks from hexagonal close-packed Co (Fig. 2a), which decrease considerably after annealing at 400°C (Fig. 2b).The latter confirms the beginning of the solid-state reaction of Co with Pt. After annealing at 500°C (Fig. 2c), the strong reflection, which can belong to the disordered (A_1CoPt(111)) or ordered ($L1_0$CoPt(111) and $L1_1$CoPt(111)) phases, appears. The high coercivity of these samples is the characteristic of $L1_0$ and $L1_1$ phases. The value $H_C \sim 8$ kOe (Fig. 1) is characteristic of the $L1_0$ phase. Therefore, it is possible to consider that in this case the magnetically hard $L1_0$CoPt(111) phase is formed in Co/Pt(111) films by solid-state synthesis.

With the increase in the annealing temperature to 600°C (Fig. 2d) and 7500°C (Fig. 2e), weak reflections identified as (111) and (222) peaks from the $CoPt_3$ phase appear. The presence of strong

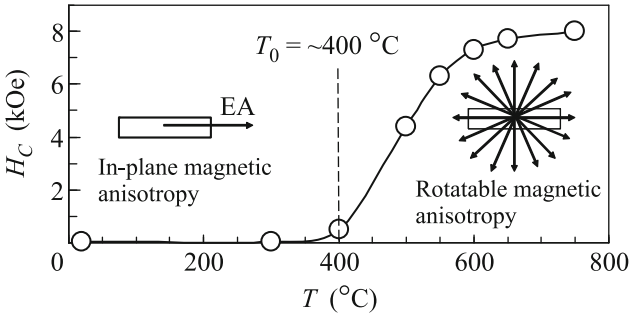

Fig. 1. Coercivity H_C Co/Pt(111) of the film system versus the annealing temperature T. The vertical dashed line shows the temperature of the initiation of the solid-state synthesis of the $L1_0$CoPt(111) phase ($T_0 \sim 400$°C).

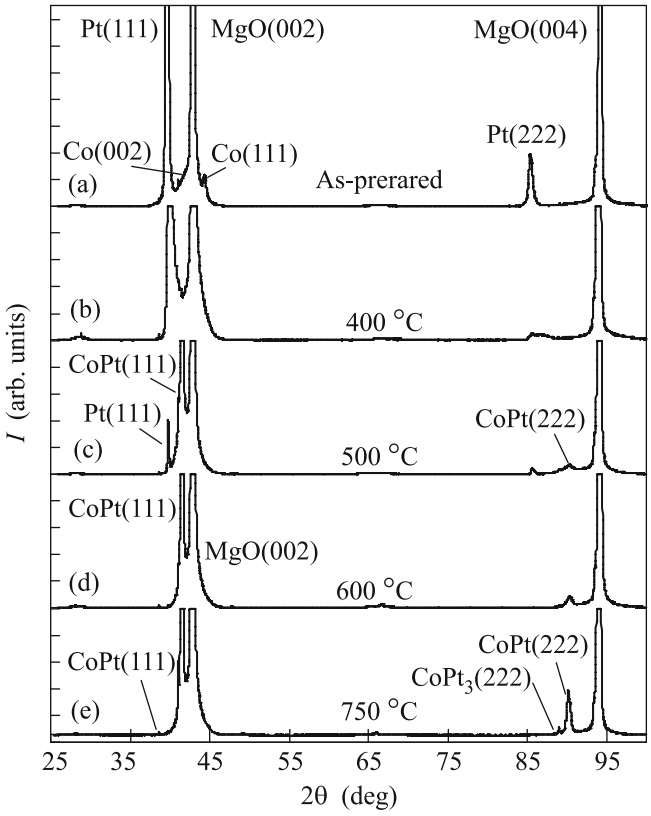

Fig. 2. X-ray diffraction patterns showing the phase transformations in the Co/Pt(111) film system at different annealing temperatures.

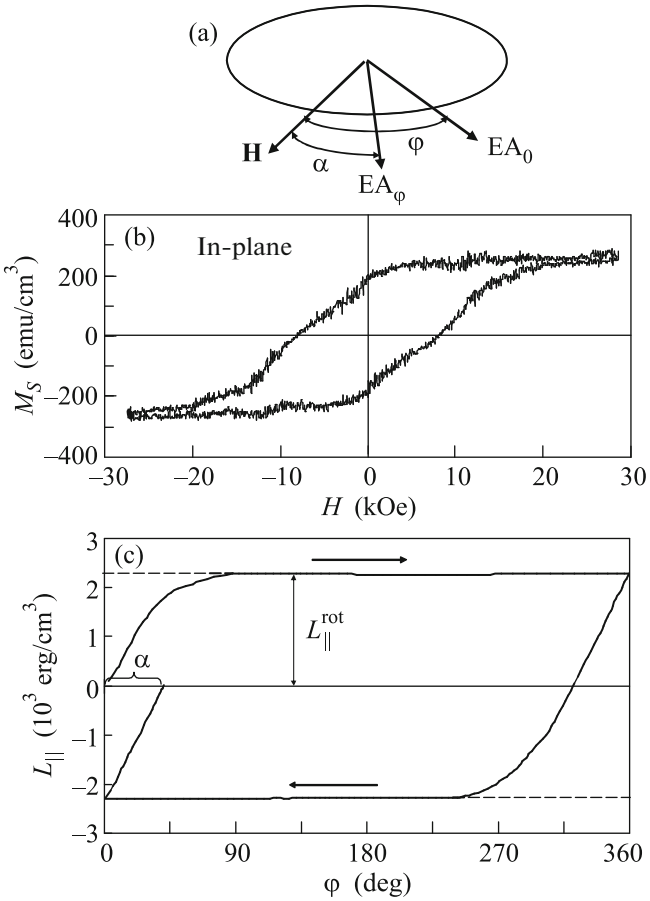

Fig. 3. (a) Schematic image, (b) $M-H$ hysteresis loop, and (c) $L_{\parallel}(\varphi)$ torque curve of the $L1_0$CoPt(111)+$CoPt_3$(111) film sample at the rotation of the magnetic field H = 10 kOe > H_C = 8 kOe by 360° (direct and reverse passes) in the sample plane. The initial easy axis EA_0 was oriented in an arbitrary direction in the film plane (a). At the rotation of the magnetic field H by the angle φ, the easy axis rotates and is established in the new position EA_φ, lagging the direction of the magnetic field H by the angle α.

($L1_0$CoPt(111) and $L1_0$CoPt(222)) and weak ((111)$CoPt_3$ and (222)$CoPt_3$) reflections indicates the epitaxial intergrowth of $L1_0$CoPt+$CoPt_3$ grains. The results of the symmetric φ scanning (not presented in this work) of (113) reflections from the MgO substrate and (311) and (211) reflections from the CoPt phases after annealing at 750°C show that $L1_0$CoPt(111) grains grow chaotically on the (001)MgO surface. Therefore, it is possible to consider that the $L1_0$CoPt+$CoPt_3$ grains having the (111) texture perpendicular to the plane and isotropic in the plane are formed at the solid-state synthesis in Co/Pt(111) of two-layer film systems. Analogous highly anisotropic $L1_0$CoPt(111) films were prepared by pulsed laser deposition on the Pt(111) sublayer preliminarily deposited on the MgO(001) substrate after annealing at 600°C [18].

Studies on the torque magnetometer showed the planar anisotropy in the initial CO/Pt(111) films, which remained to the temperature T_0 ~ 400°C of the initiation of the solid-state reaction between Co and Pt (Fig. 1). Above 400°C, the synthesis of the CoPt(111) phase started, which dramatically changed the torque curves. The torque curves acquired the shape characteristic of rotatable magnetic anisotropy after annealing above 600°C [10] and did not change their shape at 750°C. The easy axis (EA) of these samples can be built in any spatial direction in the plane and perpendicular to it (Fig. 1) taking into account the angle of the lag α of the new direction of the easy axis from the direction of the magnetic field (Figs. 3 and 4).

The structural anisotropy perpendicular to the plane and the structural in-plane anisotropy create different torque curves. Figures 3 and 4 show two variants of the torque curves under the rotation of the magnetic field H = 10 kOe by 360° (direct and reverse passages) of the CoPt(111) film having the rotatable magnetic anisotropy in the plane (Fig. 3) and in the direction perpendicular to the sample plane (Fig. 4).

(i) Since the samples are magnetically isotropic in the plane, the easy axis was oriented in an arbitrary

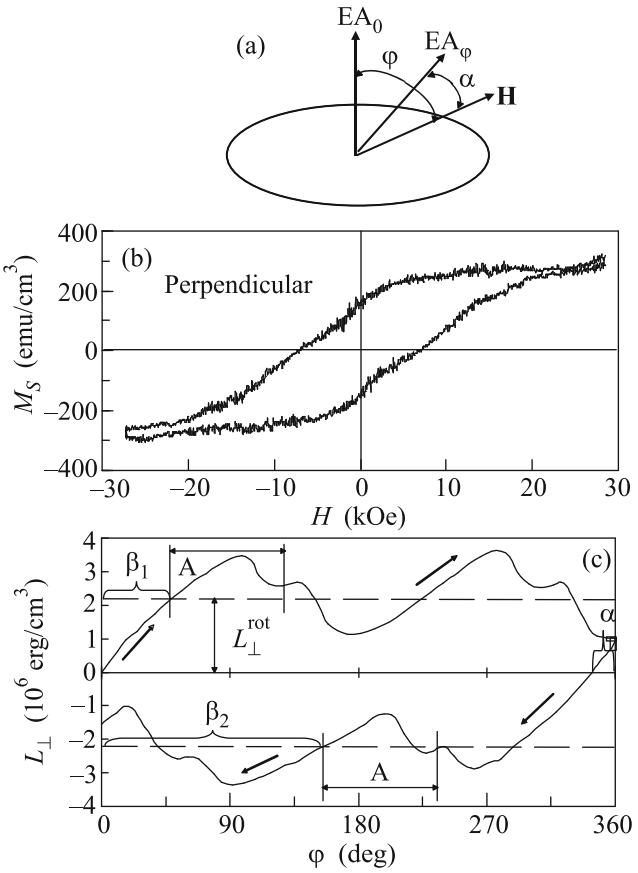

Fig. 4. (a) Schematic image, (b) M–H hysteresis loop, and (c) $L_\perp(\varphi)$ torque curve of $L1_0CoPt(111)+CoPt_3(111)$ film sample at the rotation of the magnetic field $H = 10$ kOe > $H_C = 8$ kOe by 360° (direct and reverse passes) perpendicular to the sample plane. The initial easy axis EA_0 was oriented along the normal to the film plane (a). At the rotation of the magnetic field H by the angle φ, the easy axis rotates and is established in the new position EA_φ, lagging the direction of the magnetic field H by the angle α.

direction in the plane and the magnetic field was rotated in the sample plane (Fig. 3).

(ii) The easy axis was oriented along the normal to the film and the magnetic field was rotated through the film plane (Fig. 4).

The torque curve $L_\parallel^{rot}(\varphi)$ under the rotation of the magnetic field in the plane (Fig. 3) shows the rotatable magnetic anisotropy, which is characterized by the maximum torque $L_\parallel^{rot} = 2.2 \times 10^6$ erg/cm^3 and the angle of the lag $\alpha \sim 40°$. The torque curves $L_\perp^{rot}(\varphi)$ under the rotation of the magnetic field perpendicularly to the plane (Fig. 4) can be expanded in the following components: that with the rotatable magnetic anisotropy $L_\perp^{rot} = 2.2 \times 10^6$ erg/cm^3, uniaxial with the period of 180° ($L_2 = 1 \times 10^6$ erg/cm^3), and biaxial with the period 90° ($L_4 = 0.25 \times 10^6$ erg/cm^3). In all cases, the coercivity measured along the easy axis within the experimental accuracy was constant ($H_C = 8$ kOe).

DISCUSSION OF THE RESULTS

It should be noted that all measured anisotropies are an order of magnitude less than the constants of the magnetic-crystallographic anisotropy of the $L1_0CoPt$ phase, which is the main one in the sample. The saturation magnetization of these samples M_S = 250–300 emu/cm^3 is also smaller than the value $M_S \sim$ 800 emu/cm^3 of massive samples and $L1_0CoPt$ films after annealing at 600 and 750°C [19].

The necessary condition for the easy magnetization axis to be oriented in any direction with respect to the sample plane is positive torque values $L_\perp^{rot}(\varphi)$ at the direct pass and large rotation angles φ. At the reverse pass, $L_\perp^{rot}(\varphi)$ should have negative values (see Fig. 4). The rotatable magnetic anisotropy values in the plane ($L_\parallel^{rot}$) and in the direction perpendicular to the plane ($L_\perp^{rot}$) coincide within the accuracy. The latter means that the rotatable magnetic anisotropy is a spatially isotropic characteristic of the sample. Consequently, the hysteresis loop shape and the coercivity values $H_C = 8$ kOe remain constant in any spatial direction (Figs. 3b and 4b). Thus, it is possible to conclude that the nature of perpendicular magnetic anisotropy in these samples is determined by the existence of large rotatable magnetic anisotropy.

The biaxial anisotropy with the torque $L_4 = 0.25 \times 10^6$ erg/cm^3, which appears under the rotation of the magnetic field perpendicular to the (111) plane of the sample $L1_0CoPt$, should serve as the characteristic of the cubic magnetic anisotropy. The torque curves at the direct and reverse passes have the same fragments A describing the uniaxial and biaxial anisotropies with the coinciding easy axes (Fig. 4). These axes are inclined by angles $\beta_1 \sim 135°$ and $\beta_2 \sim 45°$ to the film plane (Fig. 4). In view of a large error in the measurement of the angles β_1 and β_2, they are close to an angle of 36°, at which the [001] axes are inclined to the (111) plane in the fcc lattice. Therefore, the uniaxial and biaxial anisotropies can be attributed to the anisotropies of epitaxially intergrown and exchange-coupled $L1_0CoPt+CoPt_3$ phases, respectively. The $L1_0CoPt$ samples with the (111) textures prepared by the magnetron sputtering of the Co–Pt alloy on glass and Si(100) substrates had analogous torque curves of the rotatable magnetic anisotropy with uniaxial and biaxial anisotropies under the rotation of the magnetic field $H_C \sim 10$ kOe perpendicular to the plane [20]. However, the rotatable magnetic anisotropy in the torque curves was not detected after annealing above 600°C. This indicates that the $L1_0CoPt+CoPt_3$ films

prepared in different ways can have a high rotatable magnetic anisotropy.

A high rotatable magnetic anisotropy and low uniaxial and biaxial anisotropies and low saturation magnetization are inconsistent with the respective values for the $L1_0$CoPt phase, which is the main phase after the solid-state reaction in Co/Pt films. The possible reasons for this inconsistency can be as follows.

(i) The formation of the exchange-coupled and epitaxial intergrown $L1_0$CoPt and $L1_2CoPt_3$ nanoclusters. Such coherent two-phase mixtures $L1_0$ + $L1_2$ were found in Co–Pt alloys. They have a chessboard microstructure caused by stresses and can have magnetic properties different from those of the initial $L1_0$ and $L1_2$ phases.

(ii) The existence of the ordered L1' phase containing the hybrid ($L1_0$ + $L1_2$) structure. The L1' phase can have the magnetic characteristics intermediate between the magnetically hard ($L1_0$) and magnetically soft ($L1_2$) phases. The L1' ordering was proved experimentally in epitaxial $Fe_{38.5}Pd_{61.5}$ films [22] and was assumed in the $Co_{41.7}Pt_{58.3}$ alloy [23].

(iii) The formation of CoPt nanoparticles with the diameter of several nanometers with multiple twinning morphologies, such as an icosahedron and a decahedron containing $L1_0$ domains [24]. Such nanoparticles contain $L1_0$ domains of different orientations and, therefore, have low magnetocrystalline anisotropy [25].

It is important that the rotatable magnetic anisotropy in previous works was observed only in the sample plane. The high rotatable magnetic anisotropy, which makes it possible to orient the easy axis in any spatial direction, was observed not only in this work but also in magnetically hard δ-$Mn_{0.6}Ga_{0.4}$ films [16]. Therefore, it is possible to assume that magnetically hard $L1_0$FePt and $L1_0$FePd films near the equiatomic composition can also have a high rotatable magnetic anisotropy.

Although several models were proposed, mechanisms of the rotatable magnetic anisotropy remain unclear. Further studies are necessary for the fundamental understanding of the nature of the rotatable magnetic anisotropy.

CONCLUSIONS

In summary, the phase transitions in epitaxial Co/Pt(111) nanofilms near the equiatomic composition have been studied with the increase in the annealing temperature to 750°C. Magnetically hard $L1_0$CoPt and $CoPt_3$ phases are formed successively at the temperatures of ~400 and 600°C, respectively. After annealing at 750°C, the samples contained nanoclusters with the dominating $L1_0$CoPt(111) phase epitaxially intergrown with the $CoPt_3$(111) phase. The high rotatable magnetic anisotropy whose easy axis can be rotated in the fields exceeding the coercivity in the plane and perpendicular to the sample plane was found in the prepared samples. It was concluded that the high rotatable magnetic anisotropy can be the main source of the perpendicular anisotropy in Co_xPt_{1-x} films.

We are grateful to L.A. Solov'ev for the help in X-ray studies of the epitaxial orientation of phases in $L1_0$CoPt(111) samples. This work was supported by the Russian Foundation for Basic Research (project no. 15-02-00948), in part by the Council the President of the Russian Federation for Support of Young Scientists and Leading Scientific Schools (project no. SP-317.2015.1), and by the Foundation for the Assistance of the Development of Small Innovative Scientific and Engineering Enterprises (UMNIK).

REFERENCES

1. D. Weller, A. Moser, L. Folks, M. E. Best, W. Lee, M. F. Toney, M. Schwickert, J.-U. Thiele, and M. F. Doerner, IEEE Trans. Magn. **36**, 10 (2000), O. Gutfleisch, J. Lyubina, K.-H. Müller, and L. Schultz, Adv. Eng. Mater. **7**, 208 (2005).
2. S. D. Bader, Rev. Mod. Phys. **78**, 1 (2006), P. Andreazza, V. Pierron-Bohnes, F. Tournus, C. Andreazza-Vignolle, and V. Dupuis, Surf. Sci. Rep. **70**, 188 (2015), S. Sun, Adv. Mater. **18**, 393 (2006).
3. B. M. Lairson, M. R. Visokay, E. E. Marinero, R. Sinclair, and B. M. Clemens, J. Appl. Phys. **74**, 1922 (1993), N. Yasui, A. Imada, and T. Den, Appl. Phys. Lett. **83**, 3347 (2003), O. Ersen, V. Parasote, V. Pierron-Bohnes, M. C. Cadeville, and C. Ulhaq-Bouillet, J. Appl. Phys. **93**, 2987 (2003), L. Reichel, S. Fahler, L. Schultz, and K. Leistner, J. Appl. Phys. **114**, 093909 (2013).
4. G. Lauhoff, Y. Yamada, Y. Itoh, and T. Suzuki, J. Magn. Soc. Jpn. Suppl. SI, 43 (1999), S. C. Chen, P. C. Kuo, C. L. Shen, S. L. Hsu, and T. H. Sun, Mater. Des. **31**, 1706 (2010), K. K. M. Pandey, J. S. Chen, T. Liu, C. J. Sun, and G. M. Chow, J. Phys. D: Appl. Phys. **42**, 185007 (2009), Y. S. Chen, A.-C. Sun, H. Y. Lee, H.-C. Lu, S.-F. Wang, and P. Sharma, J. Magn. Magn. Mater. **391**, 12 (2015).
5. A.-C. Sun, C.-F. Huang, and S. H. Huang, J. Appl. Phys. **115**, 17B720 (2014), F.-T. Yuan, J.-H. Hsu, Y.-H. Lin, S. N. Hsiao, and H. Y. Lee, J. Appl. Phys. **111**, 07A303 (2012), F.-T. Yuan, A.-C. Sun, C. F. Huang, and J.-H. Hsu, Nanotechnology **25**, 165601 (2014), D. Suzuki, M. Ohtake, F. Kirino, and M. Futamoto, J. Appl. Phys. **115**, 17C120 (2014).
6. J. O. Cross, M. Newville, B. B. Maranville, C. Bordel, F. Hellman, and V. G. Harris, J. Phys.: Condens. Matter **22**, 146002 (2010), J.-J. Wang, T. Sakurai, K. Oikawa, K. Ishida, N. Kikuchi, S. Okamoto, H. Sato, T. Shimatsu, and O. Kitakami, J. Phys.: Condens. Matter **21**, 185008 (2009), J. O. Cross, M. Newville, B. B. Maranville, C. Bordel, F. Hellman, and V. G. Harris, J. Phys.: Condens. Matter **22**, 146002 (2010), J.-J. Wang, T. Sakurai, K. Oikawa, K. Ishida, N. Kikuchi, S. Okamoto, H. Sato, T. Shimatsu, and

O. Kitakami, J. Phys.: Condens. Matter **22**, 146002 (2010).

7. Y. Yamada, T. Suzuki, H. Kanazawa, and J. C. Osterman, J. Appl. Phys. **85**, 5094 (1999).
8. W. Rooney, A. L. Shapiro, M. Q. Tran, and F. Hellman, Phys. Rev. Lett. **75**, 1843 (1995), F. Liscio, M. Maret, C. Meneghini, S. Mobilio, O. Proux, D. Makarov, and M. Albrecht, Phys. Rev. B **81**, 125417 (2010), J. O. Cross, M. Newville, B. B. Maranville, C. Bordel, F. Hellman, and V. G. Harris, J. Phys.: Condens. Matter **22**, 146002 (2010).
9. D. Weller, H. Brändle, G. Gorman, C.-J. Lin, and H. Notarys, Appl. Phys. Lett. **61**, 2726 (1992), C.-Y. Tsai, P. Saravanan, J.-H. Hsu, C.-Y. Kuo, and K.-F. Lin, J. Magn. Magn. Mater. **361**, 7 (2014), H. An, J. Wang, T. Sannomiya, S. Muraishi, Y. Nakamura, and J. Shi, J. Phys. D: Appl. Phys. **48**, 155001 (2015), F. T. Yuan, H. W. Chang, P. Y. Lee, C. Y. Chang, C. C. Chi, and H. Ouyang, J. Alloys. Compd. **628**, 263 (2015).
10. R. F. Soohoo, *Magnetic Thin Films* (Harper and Row, London, 1965).
11. G. Chai, N. N. Phuoc, and C. K. Ong, Appl. Phys. Lett. **103**, 042412 (2013).
12. S. Tacchi, S. Fin, G. Carlotti, G. Gubbiotti, M. Madami, M. Barturen, M. Marangolo, M. Eddrief, D. Bisero, A. Rettori, and M. G. Pini, Phys. Rev. **89**, 024411 (2014), G. Wang, C. Dong, W. Wang, Z. Wang, G. Chai, C. Jiang, and D. Xue, J. Appl. Phys. **112**, 093907 (2012).
13. W. J. Fan, X. P. Qiu, Z. Shi, S. M. Zhou, and Z. H. Cheng, Thin Solid Films **518**, 2175 (2010), J. S. Park, J. Wu, E. Arenholz, M. Liberati, A. Scholl, Y. Meng, C. Hwang, and Z. Q. Qiu, Appl. Phys. Lett. **97**, 042505 (2010), G. Chai, N. N. Phuoc, and C. K. Ong, Sci. Rep. **2**, 832 (2012).
14. X. Liu and G. Zangari, J. Appl. Phys. **90**, 5247 (2001), M. L. Schneider, A. B. Kos, and T. J. Silva, Appl. Phys. Lett. **86**, 202503 (2005).
15. M. J. O'Shea, K. M. Lee, and A. Fert, J. Appl. Phys. **67**, 5769 (1990).
16. V. G. Myagkov, V. S. Zhigalov, L. E. Bykova, G. N. Bondarenko, Yu. L. Mikhlin, G. S. Patrin, and D. A. Velikanov, Phys. Status Solidi B **249**, 1541 (2012).
17. K. H. Ahn and S. Baika, J. Mater. Res. **17**, 2334 (2002).
18. G. Varvaro, E. Agostinelli, S. Laureti, A. M. Testa, A. Generosi, B. Paci, and V. R. Albertini, IEEE Trans. Magn. **44**, 643 (2008).
19. S. H. Liou, S. Huang, and E. Klimek, J. Appl. Phys. **85**, 4334 (1999).
20. S.-E. Park, P.-Y. Jung, and K.-B. Kim, J. Appl. Phys. **77**, 2641 (1995).
21. C. Leroux, A. Loiseau, D. Broddin, and G. Vantendeloo, Philos. Mag. B **64**, 57 (1991), Y. le Bouar, A. Loiseau, and A. G. Khachaturyan, Acta Mater. **46**, 2777 (1998), Y. Ni and A. G. Khachaturyan, Nature Mater. **8**, 410 (2009).
22. M. A. Steiner, R. B. Comes, J. A. Floro, W. A. Soffa, and J. M. Fitz-Gerald, Acta Mater. **85**, 261 (2015).
23. P. Ghatwai, E. Vetter, M. Hrdy, W. A. Soffa, and J. A. Floro, J. Magn. Magn. Mater. **375**, 87 (2015).
24. M. E. Gruner, G. Rollmann, P. Entel, and M. Farle, Phys. Rev. Lett. **100**, 087203 (2008).
25. F. Tournus, K. Sato, T. Epicier, T. J. Konno, and V. Dupuis, Phys. Rev. Lett. **110**, 055501 (2013).

Translated by L. Mosina